Mutational, NMR, and NH Exchange Studies of the Tight and Selective Binding of 8-Oxo-dGMP by the MutT Pyrophosphohydrolase†

Vibhor Saraswat, Hugo F. Azurmendi, and Albert S. Mildvan*

Department of Biological Chemistry, The Johns Hopkins University School of Medicine, 725 North Wolfe Street, Baltimore, Maryland 21205-2185

Received October 2, 2003

ABSTRACT: The solution structure of the ternary MutT enzyme−Mg^{2+}−8-oxo-dGMP complex showed the proximity of Asn119 and Arg78 and the modified purine ring of 8-oxo-dGMP, suggesting specific roles for these residues in the tight and selective binding of this nucleotide product [Massiah, M. A., Saraswat, V., Azurmendi, H. F., and Mildvan, A. S. (2003) *Biochemistry 42*, 10140−10154]. These roles are here tested by mutagenesis. The N119A, N119D, R78K, and R78A single mutations and the R78K/N119A double mutant showed very small effects on k_{cat} (≤2-fold) and K_m (≤4-fold) in the hydrolysis of dGTP, indicating largely intact active sites. $^1H-^{15}N$ HSQC spectra showed largely intact protein structures for all of these mutants. However, the N119A mutation profoundly and selectively weakened the active site binding of 8-oxo-dGMP, increasing the K_I^{slope} of this product inhibitor 1650-fold, while increasing the K_I^{slope} of dGMP and dAMP less than 2-fold. The N119D mutation also selectively weakened 8-oxo-dGMP binding but only by 37-fold, suggesting that Asn119 both donated a hydrogen bond to the C8═O group and accepted a hydrogen bond from the N7H group of 8-oxo-dGMP, while Asp119 functioned as only an acceptor. Direct binding of 8-oxo-dGMP to N119A, monitored by continuous changes in the ^{15}N and/or NH chemical shifts of 12 residues, revealed fast exchange, and a K_D of 237 ± 130 μM for 8-oxo-dGMP, comparable to its K_I^{slope} of 81 ± 22 μM. While formation of the wild-type MutT−Mg^{2+}−8-oxo-dGMP complex slowed the backbone NH exchange rates of 45 residues distributed throughout the protein, the same complex of the N119A mutant slowed the exchange rates of only 11 residues at or near the active site, indicating an increase in the conformational flexibility of the N119A mutant. The R78K and R78A mutations selectively increased the K_I^{slope} of 8-oxo-dGMP by factors of 17 and 6.6, respectively, indicating a smaller role for Arg78 than for Asn119 in the binding of 8-oxo-dGMP, likely donating a hydrogen bond to its C6═O group. The much greater contribution of Asn119 (4.0 kcal/mol) than of Arg78 (1.0 kcal/mol) to the selectivity of binding of 8-oxo-dGMP versus dGMP indicates a 2 order of magnitude smaller contribution of a structure with the reversed orientation of the 8-oxo-dG ring. The R78K/N119A double mutant weakened the binding of 8-oxo-dGMP by a factor (63 000 ± 22 000) which overlaps within error with the product of the effects of the two single mutants (28 000 ± 15 000). Such additive effects of the two single mutants in the double mutant are most simply explained by the independent functioning of Asn119 and Arg78 in the binding of 8-oxo-dGMP. Independent functioning of these two residues in nucleotide binding is consistent with their locations in the MutT−Mg^{2+}−8-oxo-dGMP complex, on opposite sides of the active site cleft, with a minimal distance of 8.4 ± 0.5 Å between their side chain nitrogens.

The MutT enzyme, a nucleoside triphosphate (NTP)[1] pyrophosphohydrolase, catalyzes the hydrolysis of NTPs to yield NMPs and inorganic pyrophosphate by nucleophilic substitution at Pβ (*1*).

$$NTP + H_2O \rightarrow NMP + PP_i + H^+ \qquad (1)$$

The solution structure (*2*, *3*) and product inhibition and mutational studies have led to kinetic (*4*) and chemical mechanisms (*5*) for this prototypical Nudix hydrolase (*6*). The best substrate for MutT is the mutagenic nucleotide 8-oxo-dGTP (*7*), which can mispair with template adenine during DNA replication (*8*, *9*). Genetic inactivation of this enzyme in *Escherichia coli* results in a 10^4-fold increase in the number of mutations, all of which are AT → CG transversions (*10*, *11*). Inactivation of a homologous 8-oxo-dGTPase in mice results in major increases in the incidence of tumors (*12*). These observations suggest that the biological role of MutT is to prevent errors in DNA replication by hydrolyzing oxidatively damaged, mutagenic nucleotides such as 8-oxo-dGTP (*7*, *12*). While the in vivo substrate of the MutT enzyme has not been unequivocally identified (*13*), 8-oxoguanine nucleotides exhibit unusually high affinities

† This research was supported by National Institutes of Health Grant DK28616 (to A.S.M.).

* To whom correspondence should be addressed. Phone: (410) 955-2038. Fax: (410) 955-5759. E-mail: mildvan@welchlink.welch.jhu.edu.

[1] Abbreviations: 8-oxo-dGMP, 8-oxodeoxyguanosine monophosphate; HSQC, heteronuclear single-quantum coherence; NMP, nucleoside monophosphate; NTP, nucleoside triphosphate; Nudix hydrolase, nucleoside diphosphate-X hydrolase; PP_i, pyrophosphate.

10.1021/bi030216o CCC: $27.50
Published on Web 03/04/2004

Chart 1

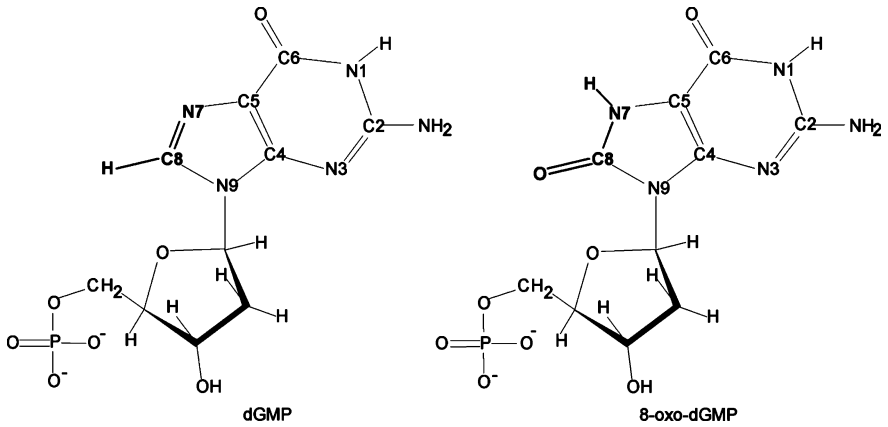

for MutT, as indicated by the low K_m of 8-oxo-dGTP (0.48 μM), which is 2300-fold lower than that of dGTP (1100 μM) (*7*), and by the 35000-fold tighter binding of the reaction product, 8-oxo-dGMP (K_D = 52 nM), than of dGMP (K_D = 1.8 mM) to the enzyme−Mg^{2+} complex (*4*).

The tight binding of 8-oxo-dGMP ($\Delta G°_{binding}$ = −9.8 kcal/mol) results from a favorable enthalpy change ($\langle \Delta H_{binding} \rangle$ = −32 kcal/mol) which exceeds an unfavorable entropy change ($\langle -T\Delta S°_{binding} \rangle$ = 22 kcal/mol), the latter indicating strong ordering in the enzyme−Mg^{2+}−8-oxo-dGMP complex (*4*). Solution structures revealed that MutT-bound nucleotides such as AMP (*3*, *14*) or 8-oxo-dGMP (*14*) made direct contact with only five or six amino acid residues, most of which were apolar, and indirect second-shell interactions with nine additional residues. Accordingly, the weak binding of dGMP at a single site perturbed the chemical shifts of 22 backbone ^{15}N and/or NH resonances, and slowed the NH exchange rates of 20 residues surrounding the nucleotide binding site (*4*, *14*). However, the tighter binding 8-oxo-dGMP at this site altered the backbone ^{15}N and/or NH chemical shifts of 62 residues and slowed the NH exchange of 45 residues throughout the protein, indicating diffuse structural changes, and overall tightening of the protein structure (*4*, *14*). Comparison of the solution structures of the MutT−Mg^{2+}−8-oxo-dGMP complex (*14*) with those of the free enzyme (*2*) and the weak MutT−Mg^{2+}(H_2O)−AMPCPP−Mg^{2+} complex (*3*) showed the structural changes induced by the binding of 8-oxo-dGMP to include movements of helix I, helix II, and loop 4 toward the nucleotide binding cleft, closing of the active site, and burying of 71−78% of the surface area of 8-oxo-dGMP (*14*).

Because of the small structural differences between 8-oxo-dGMP and dGMP (Chart 1), namely, the replacement of the purine C8H group with a C8═O group and the protonation of N7, an appropriate question to be addressed is the chemical driving force for the tight and selective binding of 8-oxo-dGMP and for the resulting diffuse conformational changes. In the solution structure of the MutT−Mg^{2+}−8-oxo-dGMP complex, the location of the bound nucleotide was defined well by 10 intermolecular NOEs between the protein and the deoxyribose ring (*14*). However, the conformation and precise orientation of bound 8-oxo-dGMP were ambiguous because of the absence of nonexchangeable protons in the modified purine ring, precluding the detection of intra- and intermolecular NOEs to the purine. Reasonable assumptions were made, namely, that the conformation (high anti) and orientation of bound 8-oxo-dGMP were very similar to those of MutT-bound dGMP and MutT-bound AMPCPP (*14*), which had previously been determined (*3*, *15*). These assumptions decreased the number of alternative orientations for bound 8-oxo-dGMP to two (Figure 1). In the first case (Figure 1A,B), bifunctional hydrogen bonding occurred between Asn119 NδH and Oδ and the C8═O and N7H groups, respectively, of 8-oxo-dGMP and monofunctional hydrogen bonding occurred from Arg78 NηH_2 (or NϵH) to the C6═O group of 8-oxo-dGMP (*14*). In the second case (Figure 1C,D), the opposite orientation of the purine ring was assumed, with Asn119 NδH and Oδ hydrogen bonded to the C6═O and N1H groups, respectively, of 8-oxo-dGMP, and with Arg78 NηH_2 (or NϵH) hydrogen bonded to the C8═O group of 8-oxo-dGMP (*14*). Indirect evidence for hydrogen bond donation by Asn119 NδH was provided by a 0.54 ppm downfield shift of its resonance on binding dGTP (*3*), and by the disappearance of both Asn119 NδH_2 resonances on binding 8-oxo-dGMP (*14*).

To resolve the orientational ambiguity of 8-oxo-dGMP, and to determine the quantitative contributions of Asn119 and Arg78 to the high affinity and specificity of MutT for 8-oxonucleotides, the effects of mutating these residues on the nucleotide binding and structural properties of MutT were investigated. A preliminary report of this work has been published (*16*).

EXPERIMENTAL PROCEDURES

Materials. The DNA mismatched primers for site-directed mutagenesis were synthesized by the DNA Analysis Facility (The Johns Hopkins University School of Medicine). The QuickChange site-directed mutagenesis kit and *E. coli* BL21-(DE3) competent cells were from Stratagene (La Jolla, CA). The QIAquick gel extraction kit and QIAGEN plasmid isolation kit were from Qiagen (Valencia, CA). The isopropyl β-D-thiogalactoside (IPTG) was from Roche (Indianapolis, IN). Tryptone and yeast extract were obtained from Difco (Detroit, MI). Ammonium sulfate, ampicillin, 2′-deoxyadenosine 5′-monophosphate, 2′-deoxyguanosine 5′-monophosphate, 2′-deoxyguanosine 5′-diphosphate, 2′-deoxyguanosine 5′-triphosphate, dithiothreitol (DTT), lysozyme, and streptomycin sulfate were from Sigma (St. Louis, MO). Vivaspin (molecular weight cutoff of 5000) centrifugal concentrators were purchased from Vivascience Limited (Gloucestershire, U.K.). The Mono Q column (HR 5/5),

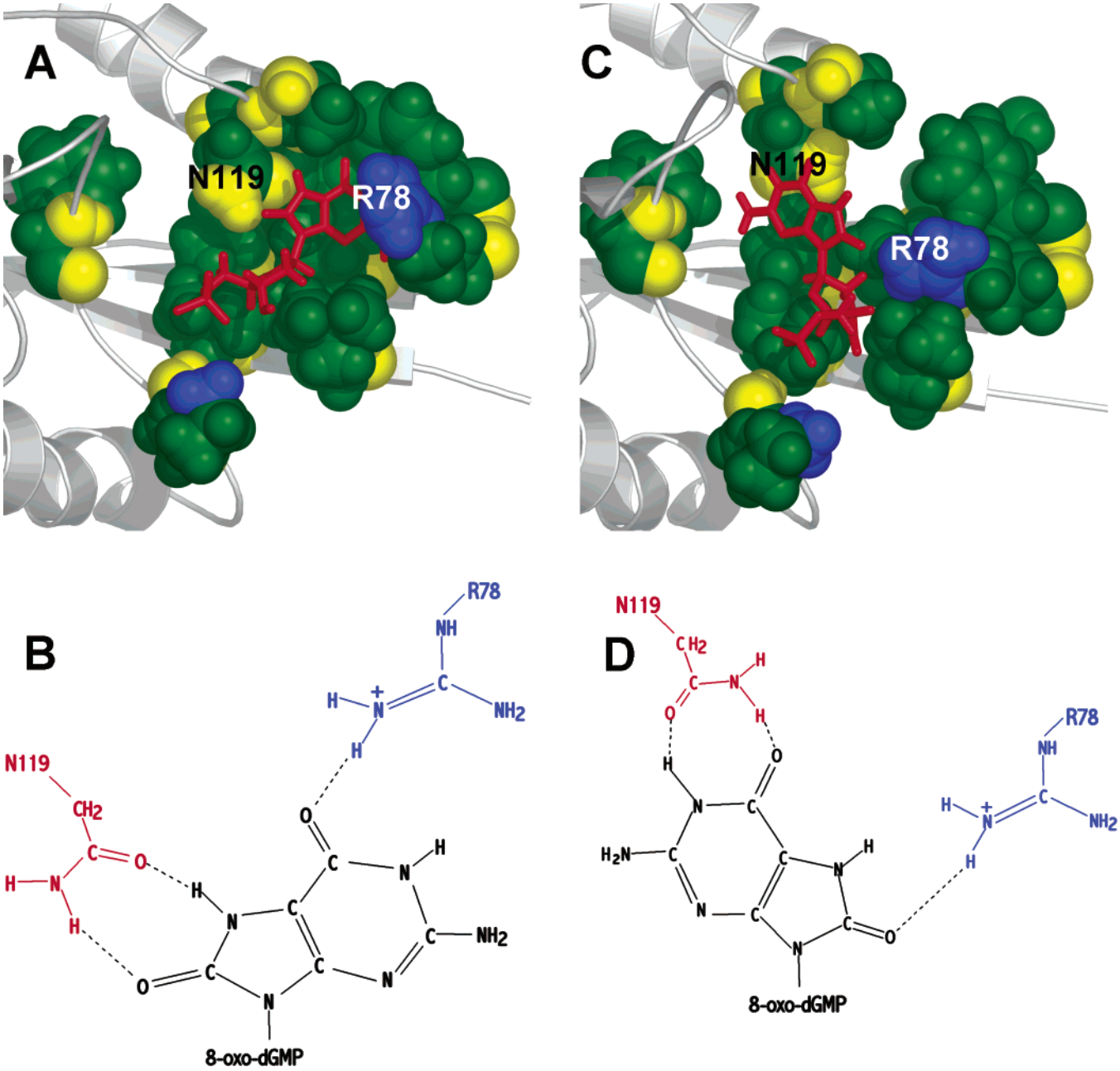

FIGURE 1: Comparison of the two alternative possible orientations for 8-oxo-dGMP bound to MutT. (A) Lowest-energy structure with bifunctional hydrogen bonding from Asn119 NδH and Oδ to the C8═O and N7H groups, respectively, of 8-oxo-dGMP and monofunctional hydrogen bonding from Arg78 NηH$_2$ to the C6═O group of 8-oxo-dGMP (case 3 in ref *14*). (B) Details of hydrogen bonding in panel A. (C) Lowest-energy structure with monofunctional hydrogen bonding from Arg78 NηH$_2$ to the C8═O group of 8-oxo-dGMP and bifunctional hydrogen bonding from Asn119 NδH and Oδ to the C6═O and N1H groups, respectively, of 8-oxo-dGMP (case 4 in ref *14*). (D) Details of hydrogen bonding in panel C.

Sephadex G-100, and DEAE-Sepharose fast-flow were from Pharmacia Biotech (Piscataway, NJ). The Microsorb 300-5 C18 HPLC column was from Dynamax-Rainin (Woburn, MA) The C18-Aqua column was from Phenomenex (Torrance, CA). Deuterium oxide (D_2O, 99.96% D) was from Aldrich (Milwaukee, WI). Uniformly (99%) ^{15}N-enriched $^{15}NH_4Cl$ was from Isotech Inc. (Miamisburg, OH). [γ-^{32}P]-ATP (4×10^6 Ci/mol) and EcoLite (+) scintillation cocktail were from ICN Biomedicals Inc. (Costa Mesa, CA). All solvents and reagents were of the highest purity available, and buffers and nucleotides were treated with Chelex-100 before they were used to remove trace metals.

Preparation of Single and Double Mutants of Arg78 and Asn119. The construction of the plasmid pETMutT, containing the MutT gene under control of the T7 promoter, has been described previously (*17*). The sequences of coding and complementary noncoding mismatch primers used for the mutations are as follows: R78A, 5′-TAT GAA TTC CCG GAC GCG CAT ATA ACA CTG TGG-3′ and 5′-CCA CAG TGT TAT ATG CGC GTC CGG GAA TTC ATA-3′; R78K, 5′-TAT GAA TTC CCG GAC AAA CAT ATA ACA CTG TGG-3′ and 5′-CCA CAG TGT TAT ATG TTT GTC CGG GAA TTC ATA-3′; N119A, 5′-GAT TTT CCG CCA GCC GCG GAA CCG GTA ATT GCG-3′ and 5′-CGC AAT TAC CGG TTC CGC GGC TGG CGG AAA ATC-3′; and N119D, 5′-GAT TTT CCG CCA GCC GAT GAA CCG GTA ATT GCG-3′ and 5′-CGC AAT TAC CGG TTC ATC GGC TGG CGG AAA ATC-3′. Each coding strand primer

and noncoding strand primer was complementary to the noncoding strand of the MutT gene, except at the appropriate mismatch (underlined) in the codon designating the amino acid to be mutated. The plasmid isolation and purification were carried out following the instruction manuals of the QIAGEN plasmid isolation kit and the QIAquick gel extraction kit, respectively. The wild-type MutT gene in the pET11b vector, [pETMutT], was used as the template for the PCR to generate the single mutants of MutT, following the instruction manual of the QuickChange site-directed mutagenesis kit.

For preparation of the R78K/N119A double mutant, the single mutant plasmid [pETMutT-R78K] was used as the template and the N119A coding and noncoding mismatch DNA oligonucleotides (see above) were used as the primers in the PCR. The mutated MutT genes in the pET11b vector were sequenced by the Johns Hopkins Medical Institutions Synthesis and Sequencing Facility. After the sequence of each mutant of MutT had been confirmed, the *E. coli* BL21-(DE3) competent cells were transformed with the plasmid having the mutant gene. The plasmid containing the mutant gene was isolated from *E. coli* BL21(DE3) cells, and the sequence of the gene was reconfirmed by DNA sequencing. With the Asn119 mutants, the mutation was also confirmed by the loss of the Asn119 $^{15}N\delta H_2$ cross-peaks from the $^1H-^{15}N$ HSQC spectrum.

Preparation of MutT. The recombinant *E. coli* HMS174-(DE3)[pETMutT] strain was used for wild-type MutT, whereas the BL21(DE3)[pETMutT-R78A], BL21(DE3)-[pETMutT-R78K], BL21(DE3)[pETMutT-N119A], BL21-(DE3)[pETMutT-N119D], and BL21(DE3)[pETMutT-R78K/N119A] strains were used for preparing uniformly ^{15}N-labeled mutants of MutT, as described previously (*5*). The enzymes were purified to >95% homogeneity on the basis of SDS−PAGE, as described previously (*5*).

Synthesis and Purification of 8-Oxo-dGMP. 8-Oxo-dGMP was synthesized and purified as described previously (*4*). The residual triethylammonium bicarbonate was removed from the 8-oxo-dGMP preparation by reverse phase HPLC using a C18-Aqua column (Phenomenex) (*14*).

General Methods. The concentration of MutT was determined spectrophotometrically using an $A_{280}^{1mg/mL}$ of 2.2 (*18*). Concentrations of dGMP, dGDP, and dGTP solutions were determined using an extinction coefficient (ϵ_{252}) of $1.37 \times 10^4\ M^{-1}\ cm^{-1}$ (*18*). Concentrations of dAMP solutions were determined using an extinction coefficient (ϵ_{260}) of $1.53 \times 10^4\ M^{-1}\ cm^{-1}$ (*19*). Concentrations of 8-oxo-dGMP were measured using an extinction coefficient (ϵ_{293}) of $1.50 \times 10^4\ M^{-1}\ cm^{-1}$ (*4*, *20*).

Kinetic Studies. [γ-^{32}P]dGTP was prepared by transphosphorylation of dGDP with [γ-^{32}P]ATP as previously reported (*5*). Steady-state kinetic experiments with Mg^{2+}-activated MutT were performed by measuring the amount of [γ-^{32}P]-pyrophosphate released from [γ-^{32}P]dGTP in Tris-HCl buffer (50 mM, pH 7.5) and 16 mM $MgCl_2$ at 23 °C (*4*). Increasing the concentration of $MgCl_2$ by 50% to 24 mM had little or no effect (≤5%), within experimental error, on the measured velocities with wild-type MutT, or with any of the mutants studied here, indicating that 16 mM $MgCl_2$ was saturating in all cases. Linear and nonlinear regression analysis of the kinetic data were performed using the program Grafit (Erithacus Software Ltd., Staines, U.K.).

$^1H-^{15}N$ HSQC Spectral Titrations of MutT with Ligands. $^1H-^{15}N$ HSQC titrations of MutT with 8-oxo-dGMP were carried out with samples containing ^{15}N-labeled R78A- or N119A-MutT (0.50 mM in R78A−8-oxo-dGMP titrations and 0.40 mM in N119A−8-oxo-dGMP titrations), 4 mM d_{11}-Tris-HCl buffer (pH 7.5), 15 mM $MgCl_2$, 21 mM NaCl, 0.33 mM sodium azide, and 10% D_2O in a total volume of 350 μL. The NMR data were collected at 23 °C on a Varian Unityplus 600 MHz NMR spectrometer equipped with *z*-axis pulsed field gradient capabilities, using a Varian 5 mm triple-resonance probe. Data were collected using the previously described pulse sequence (*21*) and processed on a Silicon Graphics Octane Workstation using NMRPipe (*22*). At each nucleotide concentration, the intensities of the protein $^1H-^{15}N$ cross-peaks were measured using the Sparky 3 software package (*23*). In titrations of the N119A mutant with 8-oxo-dGMP, the dissociation constant (K_D) for dissociation of 8-oxo-dGMP from the MutT−Mg^{2+} complex was obtained by measuring the chemical shift changes of 12 amino acid residues under conditions of fast exchange, and fitting the titration data to eq 2 by nonlinear least-squares regression analysis with the program Grafit.

$$\Delta\delta_{obs} = (\Delta\delta_{max}/2E_t)\{K_D + L_t + E_t - [(K_D + L_t + E_t)^2 - 4L_tE_t]^{1/2}\} \quad (2)$$

where L_t is the total 8-oxo-dGMP concentration, E_t is the total enzyme concentration (taking into account the small changes in enzyme concentration due to dilution upon addition of 8-oxo-dGMP), $\Delta\delta_{obs}$ is the observed chemical shift change, and $\Delta\delta_{max}$ is the chemical shift change at a saturating 8-oxo-dGMP concentration (*4*). In the MutT-R78A titration with 8-oxo-dGMP, tight nucleotide binding and slow exchange were observed at the high enzyme concentrations needed for such experiments (0.5 mM), permitting determination of only the binding stoichiometry and an upper limit to K_D.

H−D Exchange Studies. Hydrogen−deuterium exchange rates were determined at 23 °C for the N119A mutant of MutT complexed with Mg^{2+} and 8-oxo-dGMP, under conditions essentially identical to those previously used for the wild-type enzyme and its complexes (*14*). The samples contained 0.318 mM N119A-MutT, 15.0 mM $MgCl_2$, 1.49 mM 8-oxo-dGMP, 3.2 mM d_{11}-Tris-HCl (pH 7.5 in H_2O), 17 mM NaCl, and 0.45 mM NaN_3 in 10% D_2O. HSQC spectra of MutT in a 90% H_2O/10% D_2O mixture were first collected for 5 min (four scans, 64 t_1 increments, and 0.8 s relaxation delay) and 20 min (16 scans, 64 t_1 increments, and 1.0 s relaxation delay). The protein samples were then lyophilized overnight and dissolved in 99.9% D_2O to initiate the exchange, and 5 min HSQC spectra were sequentially collected for 1 h after an initial delay of 12 min for the NMR setup. Next, 20 min HSQC spectra were collected every hour for 24 h and every 3−6 h for the next 100 h. The data were processed with nmrPipe (*22*), and peak intensities were analyzed with Sparky (*23*). The ratios of the peak intensities collected for 5 and 20 min in 90% H_2O were used to normalize the intensities of peaks for data collected every 5 min in D_2O. Measurements of the decrease in peak intensities with time were fit to a one-parameter first-order equation using the Grafit 1.0 program. The NH exchange rates for each amino acid residue were then normalized with respect

Table 1: Effects of Mutations of Asn119 and Arg78 on the Kinetic[a] and Structural[b] Properties of the MutT Enzyme

enzyme	K_m (mM)	k_{cat} (s^{-1})	no. of shifted ^{15}N and NH signals/total signals
wild type[c]	0.30 ± 0.04	2.35 ± 0.12	0/115
N119A	0.07 ± 0.01	2.85 ± 0.15	19/113
N119D	0.32 ± 0.02	2.48 ± 0.06	8/114
R78A	0.13 ± 0.02	1.29 ± 0.05	14/113
R78K	1.00 ± 0.14	1.09 ± 0.08	3/115
R78K/N119A	0.29 ± 0.04	2.40 ± 0.11	21/113

[a] Kinetic parameters of the Mg^{2+}-activated hydrolysis of dGTP. [b] From $^1H-^{15}N$ HSQC spectra. [c] Data from ref *4*.

to the H−D exchange rates of free unstructured amino acids of the same type (*24*) to calculate the protection (slowing) factors, using an Excel spreadsheet provided by S. W. Englander (University of Pennsylvania, Philadelphia, PA).

RESULTS AND DISCUSSION

Effects of Mutations of Asn119 and Arg78 on the Kinetic and Structural Properties of MutT. In the standard assay of MutT with the Mg^{2+}−dGTP complex as a substrate, mutations of Asn119 and Arg78 and the double mutant R78K/N119A resulted in small or no effects on k_{cat} (≤2-fold) and K_m (≤4-fold) (Table 1), indicating that the active site is fundamentally intact.[2] Constant specific activities of these mutants after weeks of storage at −20 °C indicated stable protein structures. Intact protein structures for N119A, N119D, R78K, and R78A single mutants and for the R78K/N119A double mutant were confirmed by $^1H-^{15}N$ HSQC spectra which showed few differences between the backbone ^{15}N and NH chemical shifts and those of the wild-type enzyme, mainly near the sites of mutation (Table 1).

Product Inhibition of the N119A Mutant. Despite their largely intact protein structures, and nearly wild-type values for k_{cat} and K_m (Table 1), several of the mutants exhibited significantly weaker binding of the nucleotide products, especially 8-oxo-dGMP (Tables 2 and 3). Thus, the N119A mutation resulted in a major 1650-fold decrease in the affinity of the enzyme for 8-oxo-dGMP, as measured by the increase in K_I^{slope}, corresponding to a loss in binding free energy ($\Delta\Delta G°_{binding}$) of 4.3 kcal/mol. This weakening effect of the N119A mutation was highly selective for 8-oxo-dGMP, since dGMP and dAMP exhibited <2-fold increases in K_I^{slope}, corresponding to much smaller losses in binding free energy ($\Delta\Delta G°_{binding}$) of only 0.4 and 0.3 kcal/mol, respectively. Hence, the quantitative contribution of Asn119 to the *selectivity* of binding of 8-oxo-dGMP compared to the binding of dGMP and dAMP (Table 3) is 4.0 kcal/mol. It has previously been shown that although the binding sites of adenine and guanine nucleotides overlap, they are not identical, so the adenine ring of bound AMPCPP may not reach or interact with Asn119 (see Figure 5 of ref *14*). Because of this difference, there are no simple rules relating the affinities of adenine and guanine nucleotides for MutT.

Interestingly, the $K_I^{intercept}$ value for 8-oxo-dGMP, and for the other nucleotides, became undetectably weak, resulting in a change in the type of inhibition by nucleotide products from noncompetitive, as found with the wild-type enzyme (*4*), to competitive with the N119A mutant (Table 2). These changes indicate a change in the kinetic mechanism from iso-uni-bi in the wild-type enzyme (*4*) to simple uni-bi in the N119A mutant (*4*, *25*). In either kinetic mechanism, K_I^{slope} represents the true dissociation constant for dissociation of the nucleotide product from the enzyme−nucleotide complex (*4*, *25*).

The iso kinetic mechanism of wild-type MutT was ascribed to a partially rate-limiting interconversion of the free enzyme from the conformation which binds the NMP product to one which binds the NTP substrate (*4*). The chemical step is also partially rate-limiting in wild-type MutT as shown by pH−rate studies and by a solvent kinetic isotope effect (*5*). The change in the kinetic mechanism in the N119A mutant likely results from accelerated interconversion of the free enzyme, possibly due to its greater flexibility (see below), such that this conformational change is no longer partially rate-limiting, but chemistry remains rate-limiting. The chemical step has very similar rates in the wild-type and N119A mutant enzymes (Table 1), probably because Asn119 is far from the reaction center at Pβ of the nucleotide. Consistent with this view, the N119A mutant exhibited a slight (1.2-fold) but significant increase in k_{cat} and a 5.2-fold increase in k_{cat}/K_m (Table 1).[2]

$^1H-^{15}N$ HSQC Titration of the N119A Mutant with 8-Oxo-dGMP. The binding of 8-oxo-dGMP to the N119A mutant of MutT, in the presence of Mg^{2+}, resulted in continuous changes in the chemical shifts of backbone ^{15}N and NH resonances of 19 residues (of 113 total detected) mainly in the nucleotide binding site (Figure 2 and Table 1), indicating weak binding and fast exchange of the nucleotide on and off the enzyme at a rate exceeding the chemical shift differences between those of the free and bound enzyme. The titration data for 12 residues which showed the largest changes in chemical shifts (A7, I10, I11, E44, Q55, G59, G102, L107, L110, D113, D114, and L129) were individually fit to eq 2 (Figure 3A), yielding an average dissociation constant K_D of 237 ± 130 μM for the single nucleotide binding site on MutT. This K_D value is comparable to the kinetically determined K_I^{slope} of 8-oxo-dGMP of 81 ± 22 μM.

The titration behavior of the N119A mutant differs greatly from that of the wild-type enzyme (*4*) which, under identical conditions, showed no continuous changes in chemical shifts but, instead, continuous decreases in the intensities of 62 cross-peaks together with the appearance of 62 new cross-peaks. Such behavior indicated the tight binding and slow exchange of 8-oxo-dGMP on and off the wild-type enzyme (*4*). Accordingly, the K_D and K_I^{slope} values of 8-oxo-dGMP

[2] In an iso-uni-bi kinetic mechanism, as found with MutT (*4*), the K_m of the substrate is not a true dissociation constant, but contains at least seven rate constants (*25*). With wild-type *E. coli* MutT, at pH 7.5 and 30 °C, the K_m of the Mg^{2+}−8-oxo-dGTP complex was found to be 0.48 μM and k_{cat} was 4.2 s^{-1} (*7*). In preliminary studies with commercial 8-oxo-dGTP (Trilink Biotechnologies Inc., San Diego, CA), at the same pH (7.5) but at a lower temperature (23 °C), we confirm, by using pyrophosphatase and a sensitive colorimetric assay for phosphate (*30*), a low K_m for the Mg^{2+}−8-oxo-dGTP complex (0.52 ± 0.05 μM) and a k_{cat} of 2.8 ± 0.2 s^{-1}. With the N119A single mutant, the K_m of the Mg^{2+}−8-oxo-dGTP complex increased 317-fold to 165 μM but k_{cat} was unchanged (3.1 s^{-1}). With the R78K/N119A double mutant, the K_m of the Mg^{2+}−8-oxo-dGTP complex increased 125-fold to 65 μM and k_{cat} showed little change (4.0 s^{-1}). Hence, in contrast to the small effects of these mutations on the kinetic parameters of the hydrolysis of the Mg^{2+}−dGTP complex (Table 1), they were much more damaging to the K_m in the MutT-catalyzed hydrolysis of the Mg^{2+}−8-oxo-dGTP complex.

Table 2: Effects of Mutations of Asn119 and Arg78 on the K_I Values of NMP Products of the MutT Reaction[a]

	8-oxo-dGMP		dGMP		dAMP	
enzyme	K_I^{slope}	$K_I^{intercept}$	K_I^{slope}	$K_I^{intercept}$	K_I^{slope}	$K_I^{intercept}$
wild type	0.05 ± 0.02[b]	1.62 ± 0.88[b]	1750 ± 500[b]	14500 ± 5400[b]	4750 ± 250	30100 ± 6750
N119A	81.0 ± 21.6	−[c]	3200 ± 650	−[c]	8000 ± 1950	−[c]
N119D	1.80 ± 0.16	−[c]	6750 ± 1050	−[c]	11900 ± 1500	−[c]
R78A	0.32 ± 0.03	6.53 ± 2.44	5250 ± 500	35000 ± 7800	6500 ± 450	−[c]
R78K	0.82 ± 0.11	−[c]	5500 ± 1000	45800 ± 1100	13950 ± 500	35800 ± 4850
R78K/N119A	3100 ± 500	−[c]	12400 ± 1600	24600 ± 4700	22800 ± 7800	153000 ± 21900

[a] All K_I values are in micromolar. [b] Data from ref *4*. [c] No intercept effects were detected.

Table 3: Factors by Which the K_I^{slope} and $K_I^{intercept}$ of Nucleotides Increase and Increases in the Free Energies of Binding of Nucleotides to Mutants of MutT[a]

	8-oxo-dGMP			dGMP			dAMP		
enzyme	K_I^{slope} (fold increase)	$K_I^{intercept}$ (fold increase)	$\Delta\Delta G°_{binding}$ (kcal/mol)	K_I^{slope} (fold increase)	$K_I^{intercept}$ (fold increase)	$\Delta\Delta G°_{binding}$ (kcal/mol)	K_I^{slope} (fold increase)	$K_I^{intercept}$ (fold increase)	$\Delta\Delta G°_{binding}$ (kcal/mol)
wild type	1.0	1.0	0	1.0	1.0	0	1.0	1.0	0
N119A	1650 ± 670	−	4.3 ± 0.3	1.84 ± 0.63	−	0.36 ± 0.21	1.69 ± 0.42	−	0.31 ± 0.15
N119D	36.7 ± 11.7	−	2.1 ± 0.2	3.87 ± 1.24	−	0.79 ± 0.20	2.52 ± 0.34	−	0.54 ± 0.08
R78A	6.6 ± 2.1	4.03 ± 2.6	1.1 ± 0.2	3.01 ± 0.90	2.42 ± 1.05	0.64 ± 0.18	1.38 ± 0.11	−	0.19 ± 0.05
R78K	16.8 ± 5.6	−	1.7 ± 0.2	3.14 ± 1.06	3.16 ± 1.18	0.67 ± 0.20	2.96 ± 0.17	1.19 ± 0.31	0.63 ± 0.04
R78K/N119A	63300 ± 21900	−	6.5 ± 0.2	7.13 ± 2.20	1.69 ± 0.70	1.15 ± 0.18	4.80 ± 1.66	5.09 ± 1.35	0.92 ± 0.21

[a] Derived from the data in Table 2.

were 52 ± 13 and 49 ± 15 nM, respectively, for wild-type MutT (*4*), indicating that the binding of 8-oxo-dGMP to the wild-type enzyme was tighter by 3 orders of magnitude than the binding to N119A (Table 3).

H−D Exchange Studies of the N119A Mutant Complexed with Mg^{2+} and 8-Oxo-dGMP. We have previously shown that the tight binding of 8-oxo-dGMP to wild-type MutT is accompanied by a change in tertiary structure which narrows the nucleotide binding cleft (*14*). Widespread conformational changes in the protein also occur (*4*), resulting in a general tightening of the protein structure, as detected by the slowed H−D exchange of the backbone NH resonances of 45 residues after 62 h in D_2O (*14*). To determine the effects of the mutation most damaging to the binding of 8-oxo-dGMP on the tightness of the protein structure, we studied the NH exchange behavior of the N119A−Mg^{2+}−8-oxo-dGMP complex. After 62 h of exchange in D_2O under conditions essentially identical to those used with the wild-type enzyme (*14*), the N119A mutant slowed the NH exchange of only 11 residues, indicating a much more flexible protein structure in the N119A mutant. All of the 11 residues strongly protected against exchange in the mutant were in or near the active site (I10 and I11 in β-strand A, L54 in helix I, F68 near β-strand C, and I80, L82, W83, F84, W85, L86, and V87 in β-strand D), suggesting that these residues were directly protected at least in part by the bound nucleotide. Ten of these 11 residues, excluding L54, were among the 45 residues protected against exchange in the 8-oxo-dGMP complex of the wild-type enzyme. Hence, the N119A mutation accelerated the NH exchange of 35 residues throughout the protein, consistent with greater conformational flexibility in this mutant.

Exchange Rate Protection Factors for the N119A−Mg^{2+}−8-Oxo-dGMP Complex. Pseudo-first-order rate constants for the NH exchange of the assigned resonances at 23 °C were calculated and compared with exchange rate constants of the same residues exposed to solvent in small peptides to yield protection (or slowing) factors (*14*, *24*). The log(protection factors) vary from 0 (red), indicating no protection, to 6.4 (violet), indicating significant protection (Figure 4). A comparison of the protection factors of the wild type−Mg^{2+}−8-oxo-dGMP complex (Figure 4A) (*14*) with those of the N119A−Mg^{2+}−8-oxo-dGMP complex (Figure 4B) indicates significant decreases in protection factors in the complex of the mutant distributed throughout the protein structure. A more detailed and quantitative comparison of the exchange properties of the N119A mutant with wild-type MutT is seen in the differences in log(protection factors) (Figure 4C) which are equal to the log(ratios) of the protection factors of mutant and wild-type enzymes when both are complexed with Mg^{2+} and 8-oxo-dGMP. Most residues of the N119A mutant exhibit decreases in the protection factors of 1−4 orders of magnitude from those of the wild-type enzyme. The only exceptions are I11, K39, and H79 which exhibit slightly greater protection in the mutant.

Properties of the N119D Mutant. A 37-fold decrease in the affinity for 8-oxo-dGMP, in comparison with that of wild-type MutT, was found with the N119D mutant, as measured by the increase in K_I^{slope} (Table 3), corresponding to a loss of binding free energy ($\Delta\Delta G°_{binding}$) of 2.1 kcal/mol, half of the binding free energy lost in the N119A mutant. As with N119A, the weakening effect of the N119D mutation was selective for 8-oxo-dGMP, with order of magnitude smaller weakening effects on the binding of dGMP (3.9-fold) and dAMP (2.5-fold) (Table 3). As also found with N119A, the type of nucleotide product inhibition with N118D was competitive, unlike the noncompetitive inhibition found with wild-type MutT (*4*), indicating a change in the kinetic mechanism in the N119D mutant to simple uni-bi, presumably due to the greater conformational flexibility of the protein, as discussed above for N119A.

While the side chain of asparagine can simultaneously both donate and accept hydrogen bonds, that of aspartate can only accept a hydrogen bond. Hence, the residual binding

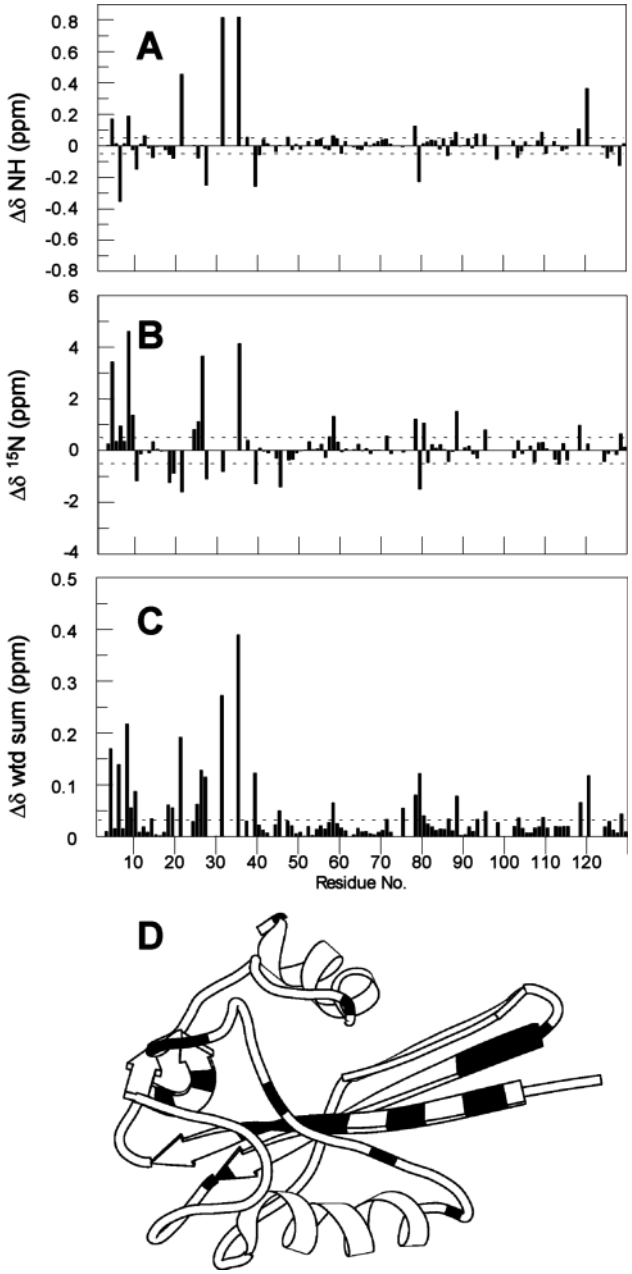

FIGURE 2: Effects of 8-oxo-dGMP binding on the backbone ^{15}N and NH chemical shifts of the N119A mutant of MutT complexed with Mg^{2+}. Chemical shift differences ($\Delta\delta = \delta$[N119A−Mg^{2+}−8-oxo-dGMP] − δ[N119A−Mg^{2+}]) were calculated on the basis of the chemical shift values obtained from $^1H-^{15}N$ HSQC spectra and are plotted vs residue number. (A) NH chemical shift differences. (B) ^{15}N chemical shift differences. (C) Sum of the absolute magnitudes of the ^{15}N and NH chemical shift changes which were weighted according to the backbone amide chemical shift dispersion in the ^1H (3.38 ppm) and ^{15}N (28.586 ppm) dimensions of the N119A−Mg^{2+} spectra. In panels A−C, the dashed lines indicate the error levels in $\Delta\delta$. (D) Sites of backbone NH and/or ^{15}N chemical shift differences (at least twice the error limits) between the N119A−Mg^{2+}−8-oxo-dGMP and N119A−Mg^{2+} complexes are shaded black. Samples contained 0.40 mM N119A-MutT, 15.0 mM $MgCl_2$, 21 mM NaCl, 0.33 mM NaN_3, and 4.0 mM d_{11}-Tris-HCl [pH 7.5, in 10% (v/v) D_2O]. $T = 23$ °C.

selectivity of 1.3 kcal/mol of the N119D mutant for 8-oxo-dGMP ($\Delta\Delta G°_{binding} = 2.1$ kcal/mol) versus dGMP ($\Delta\Delta G°_{binding} = 0.8$ kcal/mol) (Table 3) could well result from Asp119 accepting a single hydrogen bond from N7H of 8-oxo-dGMP. The 42-fold greater weakening of 8-oxo-dGMP binding by the N119A than by the N119D mutation, corresponding to a 2.2 kcal/mol greater loss in binding free energy, and the selective effects on 8-oxo-dGMP binding by these mutations support the bifunctional interaction of Asn119 with 8-oxo-dGMP, in the manner shown in panels A and B of Figure 1, rather than as in panels C and D.

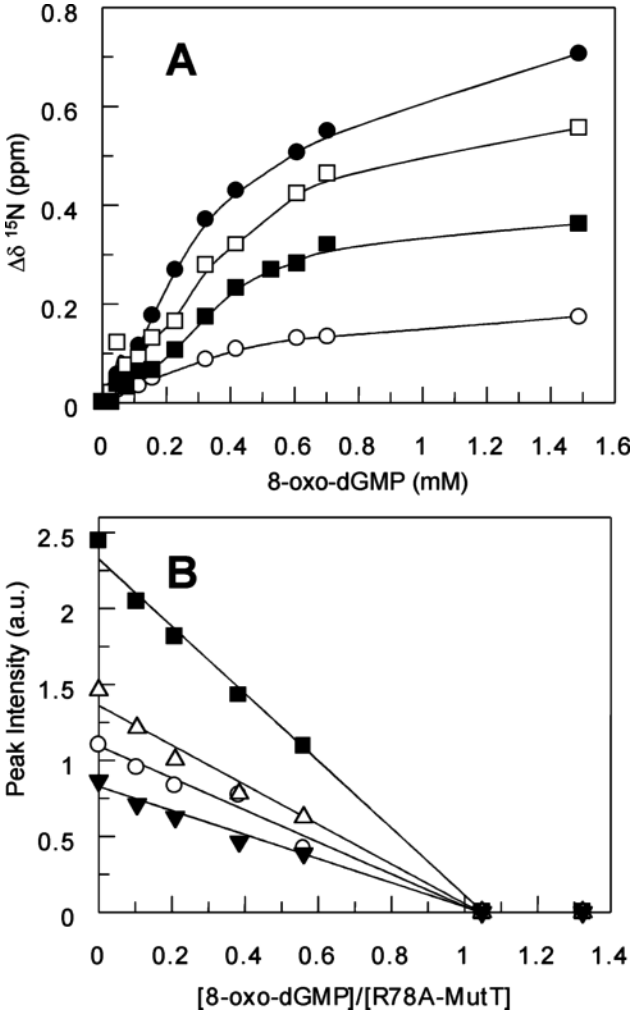

FIGURE 3: $^1H-^{15}N$ HSQC titrations of mutants of MutT with 8-oxo-dGMP in the presence of a saturating Mg^{2+} concentration. (A) Determination of the K_D of 8-oxo-dGMP by titrations of the N119A mutant of MutT (0.40 mM N119A and 15 mM $MgCl_2$) with 8-oxo-dGMP by plotting the changes in ^{15}N chemical shifts of G59 (■), L107 (□), D113 (●), and L129 (○) vs 8-oxo-dGMP concentration. (B) Determination of the stoichiometry of binding of 8-oxo-dGMP to the R78A mutant of MutT. Plots of peak intensity of R12 (○), L82 (■), L85 (△), and L86 (▼) vs [8-oxo-dGMP]/[N119A-MutT] molar ratios. Peak intensities were obtained from the $^1H-^{15}N$ HSQC titration of R78A (0.50 mM) with 8-oxo-dGMP, in the presence of 15 mM $MgCl_2$ at 23 °C. Other components and conditions were as described in the legend of Figure 2.

Properties of Mutants of Arg78. The largely intact R78K mutation (Table 1) weakens 8-oxo-dGMP binding 17-fold, corresponding to a $\Delta\Delta G°_{binding}$ of 1.7 kcal/mol, with smaller (3-fold) effects on dGMP and dAMP binding (Tables 2 and 3), indicating a smaller role for Arg78 than for Asn119 in the selective binding of 8-oxo-dGMP. The 1.0 kcal/mol difference in the contributions of Arg78 to the binding of 8-oxo-dGMP (1.7 kcal/mol) and dGMP (0.7 kcal/mol) is a measure of the contribution of Arg78 to *selectivity*. Hence, Asn119 plays a much larger role than Arg78 in both the binding of 8-oxo-dGMP (4.3 kcal/mol vs 1.7 kcal/mol) and

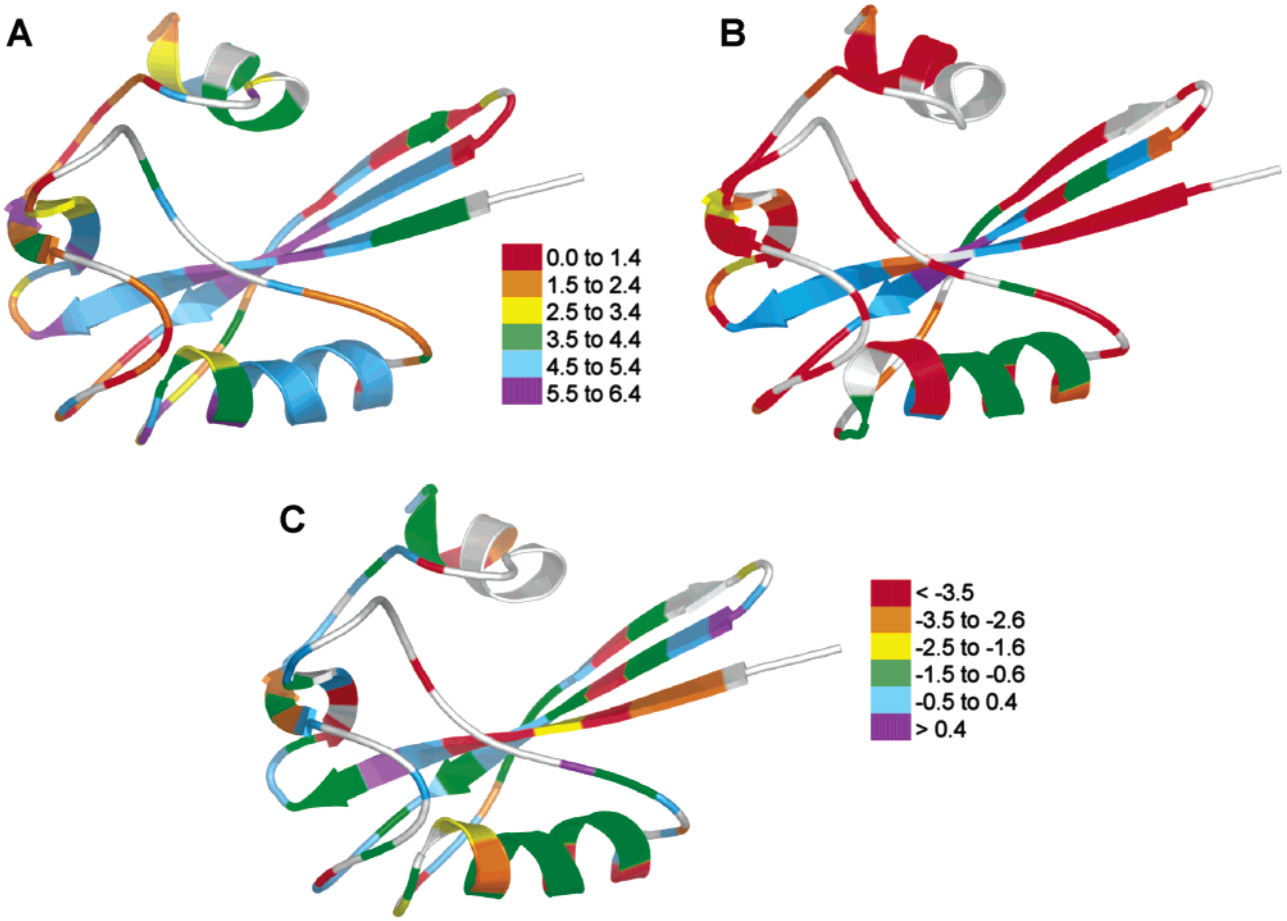

FIGURE 4: Protection (slowing) factors for backbone NH−ND exchange, at pH 7.5 and 23 °C, of individual residues for 8-oxo-dGMP complexes of MutT: (A) wild-type MutT−Mg^{2+}−8-oxo-dGMP complex (*14*) and (B) N119A−Mg^{2+}−8-oxo-dGMP complex. The color code indicates log[protection factors], ranging from red, for little or no protection, to violet, for residues protected ≥10^6-fold (i.e., for more than 7 days). (C) Difference between the log[protection factors] of the N119A−Mg^{2+}−8-oxo-dGMP and wild-type MutT−Mg^{2+}−8-oxo-dGMP complexes. Residues with enhanced protection in the mutant complex vs the wild type are colored violet, and those with equal protection are colored blue. Progressively decreasing protection factors in a comparison of the mutant vs the wild type are shown in green, yellow, orange, and red.

selectivity of MutT for 8-oxo-dGMP versus dGMP (4.0 kcal/mol vs 1.0 kcal/mol) (Table 3). The 2.6 kcal/mol greater contribution by Asn119 to the binding of 8-oxo-dGMP is consistent with bifunctional hydrogen bonding between Asn119 and the purine ring of 8-oxo-dGMP, and monofunctional hydrogen bonding by Arg78 (Figure 1).

The 3.0 kcal/mol greater contribution of Asn119 to the *selectivity* for 8-oxo-dGMP over dGMP suggests a 170-fold greater contribution of the structure shown in panels A and B of Figure 1 than that shown in panels C and D. A larger estimate of this ratio is provided by the R78A mutation (see below). In the predominant structure, Asn119 both donates a hydrogen bond to the C8═O group and accepts a hydrogen bond from the N7H group of 8-oxo-dGMP, while Arg78 donates a hydrogen bond to the C6═O group which does not contribute to *selectivity*. Hence, a much smaller contribution of the opposite orientation of bound 8-oxo-dGMP (Figure 1C,D) to the overall structure of the complex would explain the small 1.0 kcal/mol contribution of Arg78 to the *selectivity* for 8-oxo-dGMP, namely, by donating a single hydrogen bond to the C8═O group. In this minor species, Asn119 does not contribute to selectivity since it interacts with the N1H and C6═O groups of 8-oxo-dGMP.

As with wild-type MutT, both dGMP and dAMP showed noncompetitive inhibition of R78K, consistent with a partially rate-limiting conformational interconversion of the free enzyme in an iso mechanism (*4*, *25*). Consistent with an additional slow step, the k_{cat} of the R78K mutant was 2.2-fold lower than that of the wild-type enzyme (Table 1). As previously noted, the $K_I^{intercept}$, when measurable, is difficult to interpret quantitatively because it contains both kinetic and equilibrium terms, and the kinetic terms both multiply and add to the dissociation constant of the nucleotide (*4*, *25*). The tighter binding 8-oxo-dGMP showed simple competitive inhibition of R78K, reflecting a more facile conformational interconversion in the binding of this preferred nucleotide to the R78K mutant.

Surprisingly, the R78A mutation was less damaging to the binding of 8-oxo-dGMP (6.6-fold increase in K_I^{slope}) than the more conservative R78K mutation (17-fold increase in K_I^{slope}), reinforcing the modest role of Arg78 in the binding of 8-oxo-dGMP. The R78A mutation showed a smaller 3-fold effect on dGMP binding but showed little effect on dAMP binding (Table 2). The R78A mutation also preserved noncompetitive inhibition by 8-oxo-dGMP and dGMP, but not by dAMP (Table 2).

The R78A mutant exhibited an only 0.5 kcal/mol contribution of Arg78 to the *selectivity* for 8-oxo-dGMP which is 3.5 kcal/mol smaller than that of Asn119 (Table 3), suggesting a 400-fold greater contribution of the structure shown

in panels A and B of Figure 1 than that shown in panels C and D to the MutT−Mg^{2+}−8-oxo-dGMP complex. The 2.4-fold greater contribution of the structure in panels A and B found with R78A than with R78K may result from the loss of the electrostatic effect of a lysine at position 78.

$^1H-^{15}N$ HSQC titration of the R78A mutant with 8-oxo-dGMP showed decreases in the intensities of resonances and the appearance of new resonances, rather than continuous changes in chemical shifts, indicating slow exchange and tight binding of 8-oxo-dGMP, in accord with its low K_I^{slope} of 324 ± 27 nM (Table 2). The binding of 8-oxo-dGMP to the R78A mutant perturbed the backbone ^{15}N and NH chemical shifts of 46 residues (of 113 signals) widely distributed throughout the protein (Figure 5), similar to the findings with the wild-type enzyme (*4*). Plots of resonance intensities as a function of 8-oxo-dGMP concentration for 21 signals (exemplified in Figure 3B) yielded tight, stoichiometric binding to 1.03 ± 0.04 sites on the enzyme. In such cases of tight binding ligands, with K_D values much lower than the protein concentration needed for HSQC titrations, one can obtain only a binding stoichiometry but not a dissociation constant (*4*). The protein concentration that was used (0.50 mM) sets a high upper limit on K_D (*4*).

Properties of the R78K/N119A Double Mutant. The single mutations of Arg78 and Asn119 which were most damaging to the binding of 8-oxo-dGMP were combined in the R78K/N119A double mutant. This double mutant exhibited k_{cat} and K_m values for dGTP that were indistinguishable from those of the wild-type enzyme (Table 1), indicating an intact active site. The $^1H-^{15}N$ HSQC spectrum showed chemical shift changes for 21 of 113 detectable resonances (Table 1), predominantly surrounding the sites of the two mutations, indicating an otherwise intact protein structure. However, as measured by the increases in K_I^{slope}, the R78K/N119A double mutant weakened 8-oxo-dGMP binding 63000-fold, while the single mutants R78K and N119A weakened 8-oxo-dGMP binding by factors of 17 and 1650, respectively (Tables 2 and 3). Within experimental error, the product of the effects of the two single mutants on the K_I^{slope} of 8-oxo-dGMP (28 000 ± 15 000) overlaps with the effect of the double mutant on this parameter (63 000 ± 22 000). Hence, the losses of binding free energy for 8-oxo-dGMP caused by the N119A single mutant ($\Delta\Delta G°_{binding}$ = 4.3 ± 0.3 kcal/mol) and the R78K single mutant ($\Delta\Delta G°_{binding}$ = 1.7 ± 0.2 kcal/mol) were additive in the double mutant ($\Delta\Delta G°_{binding}$ = 6.5 ± 0.2 kcal/mol). Similarly, the much smaller decreases in the affinity of MutT for dGMP and dAMP in the single mutants also show additivity in the double mutant (Table 3). Such additivities of the effects of the two single mutations on $\Delta\Delta G°_{binding}$ in the double mutant are most simply explained by the independent functioning of Asn119 and Arg78 in the binding of 8-oxo-dGMP, dGMP, and dAMP (*26*). The independent functioning of Asn119 and Arg78 in the binding of nucleotides is consistent with them being somewhat remote from each other, on opposite sides of the nucleotide binding cleft, with side chain N---N distances between Asn119 NδH_2 and Arg78 NηH_2 of 8.4 ± 0.5 Å in the 8-oxo-dGMP complex (Figure 1) (*14*).

While $\Delta\Delta G°_{binding}$ shows the additive effects of the N119A and R78K mutations for the three nucleotides that were studied (Table 3), the interactions of the effects of these mutations on $\Delta\Delta H_{binding}$ and on $-T\Delta\Delta S°_{binding}$ are unknown and may not be additive in view of the increased flexibility of the N119A mutant compared to that of the wild-type enzyme (Figure 4). Such effects will be investigated by calorimetry.

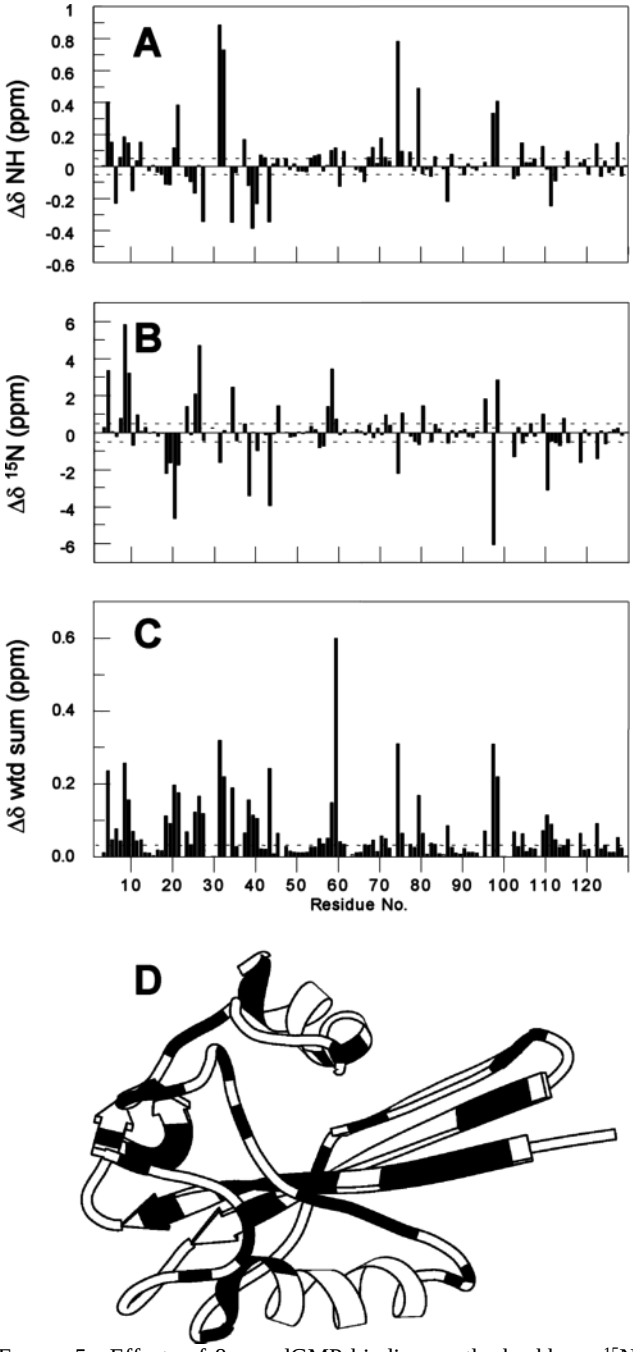

FIGURE 5: Effects of 8-oxo-dGMP binding on the backbone ^{15}N and NH chemical shifts of the R78A mutant of MutT complexed with Mg^{2+}. Chemical shift differences ($\Delta\delta = \delta$[R78A−Mg^{2+}−8-oxo-dGMP] − δ[R78A−Mg^{2+}]) were calculated on the basis of the chemical shift values obtained from $^1H-^{15}N$ HSQC spectra and are plotted vs residue number. (A) NH chemical shift differences. (B) ^{15}N chemical shift differences. (C) Sum of the absolute magnitudes of the ^{15}N and NH chemical shift changes which were weighted according to the backbone amide chemical shift dispersion in the ^1H (3.38 ppm) and ^{15}N (28.586 ppm) dimensions of the R78A−Mg^{2+} spectra. (D) Sites of backbone NH and/or ^{15}N chemical shift differences (at least twice the error limits) from R78A−Mg^{2+}−8-oxo-dGMP and R78A−Mg^{2+} complexes are shaded black. Samples contained 0.50 mM R78A-MutT, 15.0 mM $MgCl_2$, 0.33 mM NaN_3, and 4.0 mM d_{11}-Tris-HCl [pH 7.5, in 10% (v/v) D_2O]. T = 23 °C.

The R78K/N119A double mutant weakens the binding of 8-oxo-dGMP by 6.5 kcal/mol, but weakens the binding of dGMP by only 1.1 kcal/mol (Table 3), indicating a *selective* effect of the two mutations of 5.4 kcal/mol on 8-oxo-dGMP binding. The magnitude of this selective effect approaches the 6.1 kcal/mol greater affinity of the wild-type enzyme for 8-oxo-dGMP than for dGMP (*4*). These data suggest that Asn119 and Arg78, functioning predominantly as shown in panels A and B of Figure 1, with a 2 order of magnitude smaller contribution of the structure shown in panels C and D, provide the major driving force for the tighter and selective binding of 8-oxo-dGMP by the wild-type enzyme, and for the resulting conformational changes (*14*). Like the R78K single mutant, the R78K/N119A double mutant preserved noncompetitive inhibition by dGMP and dAMP. Like both the R78K and N119A single mutants, the double mutant showed simple competitive inhibition by 8-oxo-dGMP (Table 2), consistent with the greater conformational flexibility of this mutant when it interacts with its preferred ligand.

Finally, it is noted that the important roles of Arg78 and Asn119, found here to provide the structural basis for the selective binding of 8-oxo-dGMP by *E. coli* MutT, are not universal (*27*−*29*), even among MutT homologues (*27*). Thus, in the human, mouse, and rat homologues of MutT, Arg78 is replaced with Ser and Asn119 is replaced with Asp (*27*). Unlike *E. coli* MutT, these homologous enzymes hydrolyze 2-oxo-dATP as well as 8-oxo-dGTP, and Asp119 plays a significant role in the binding of 2-oxo-dATP but not of 8-oxo-dGTP in these homologues (*27*). Despite this observation, the N119D mutant of *E. coli* MutT did not acquire 2-oxo-dATPase activity (*27*). Further, Trp117 is conserved among mammalian MutT homologues, and the W117A mutation of the human homologue of MutT decreased both 2-oxo-dATPase and 8-oxo-dGTPase activities by at least 1 order of magnitude, suggesting the importance of aromatic stacking in these homologues (*27*). However, in *E. coli* MutT, Trp117 is replaced with Pro. Although the purine rings of bound nucleotides approach Tyr73 and Phe75 in *E. coli* MutT (*3*, *14*), they do not stack onto them. Hence, other species appear to have evolved different strategies for recognizing several mutagenic nucleotides with the same enzyme, while preserving enough selectivity to minimize the hydrolysis of essential nucleotides. *E. coli* MutT uses Asn119 and Arg78 to provide high selectivity only for 8-oxo-dGTP.

CONCLUSIONS

To evaluate the quantitative contributions of Asn119 and Arg78 to the tight and selective binding of 8-oxo-dGMP by the MutT enzyme from *E. coil*, and to clarify the precise orientation of bound 8-oxo-dGMP with respect to these residues, the effects of mutating them were studied. Asn119 makes a major 1650-fold contribution to the binding of 8-oxo-dGMP by the MutT enzyme on the basis of the weakening effects of the N119A mutation on the K_I^{slope} and K_D of this nucleotide. The smaller 37-fold weakening effect of the N119D mutation suggests that Asn119 acts bifunctionally by both donating a hydrogen bond to the C8═O group and accepting a hydrogen bond from the N7H group of 8-oxo-dGMP (Figure 1A,B) while Asp119 acts monofunctionally by accepting a hydrogen bond from the N7H group. Much smaller effects of these mutations on the K_I^{slope} of dGMP (1.8−4-fold) and dAMP (1.7−2.5-fold) are found, establishing the selectivity of these effects on the binding of 8-oxo-dGMP. Quantitatively, Asn119 contributes 4.0 kcal/mol to the *selectivity* of binding of 8-oxo-dGMP versus dGMP.

Arg78 makes a much smaller 6.6−17-fold contribution to the binding of 8-oxo-dGMP than Asn119 does, probably by donating a hydrogen bond to the C6═O group (Figure 1A,B), and a much smaller contribution of 0.5−1.0 kcal/mol to the *selectivity* of binding of 8-oxo-dGMP versus dGMP. These data are consistent with a major contribution of the structure shown in panels A and B of Figure 1 and a 2 order of magnitude smaller contribution of the structure shown in panels C and D of Figure 1 in which Arg78 makes a small contribution to *selectivity*.

The effects of the R78K and N119A single mutations on the K_I^{slope} of 8-oxo-dGMP were additive in the double mutant, suggesting that Asn119 and Arg78 function independently in the binding of 8-oxo-dGMP. The quantitative contribution of these two residues to the selective binding of 8-oxo-dGMP versus dGMP (5.4 kcal/mol) approaches the 6.1 kcal/mol greater affinity of MutT for 8-oxo-dGMP over dGMP and dAMP (*4*) (Tables 2 and 3), suggesting that these residues provide the major driving force for the tighter binding of 8-oxo-dGMP and for the resulting conformational changes (*14*).

Another effect of the N119A mutation, detected in its ternary complex with Mg^{2+} and 8-oxo-dGMP, is the accelerated backbone NH exchange of 35 residues widely distributed throughout the protein, indicating a conformationally more flexible protein. The increased protein flexibility of the N119A mutant and of the other mutants can explain the loss of intercept effects in the product inhibition by nucleotides (Tables 2 and 3), indicating a change in the kinetic mechanism from iso-uni-bi in wild-type MutT to simple uni-bi in the mutants. Greater protein flexibility would facilitate the conformational interconversion of the free enzyme from the form which binds the NMP product to the form which binds the NTP substrate, removing this conformational change as the partially rate-limiting "iso" step in the reaction, and thereby abolishing the iso mechanism.

Other enzymes which selectively bind 8-oxo-dG nucleotides (*27*−*29*), including mammalian homologues of MutT (*27*), use different structural approaches to achieve the selective binding of oxidized nucleotides.

ACKNOWLEDGMENT

We are grateful to Dr. Michael A. Massiah for his help with the NMR instrumentation.

REFERENCES

1. Mildvan, A. S., Weber, D. J., and Abeygunawardana, C. (1999) Solution structure and mechanism of the MutT pyrophosphohydrolase, *Adv. Enzymol. Relat. Areas Mol. Biol. 73*, 183−207.
2. Abeygunawardana, C., Weber, D. J., Gittis, A. G., Frick, D. N., Lin, J., Miller, A.-F., Bessman, M. J., and Mildvan, A. S. (1995) Solution structure of the MutT enzyme, a nucleoside triphosphate pyrophosphohydrolase, *Biochemistry 34*, 14997−15005.
3. Lin, J., Abeygunawardana, C., Frick, D. N., Bessman, M. J., and Mildvan, A. S. (1997) Solution structure of the quaternary MutT-M^{2+}-AMPCPP-M^{2+} complex and mechanism of its pyrophosphohydrolase action, *Biochemistry 36*, 1199−1211.
4. Saraswat, V., Massiah, M. A., Lopez, G., Amzel, L. M., and Mildvan, A. S. (2002) Interactions of the products 8-oxo-dGMP,

dGMP, and pyrophosphate with the MutT nucleoside triphosphate pyrophosphohydrolase, *Biochemistry 41*, 15566−15577.
5. Harris, T. K., Wu, G., Massiah, M. A., and Mildvan, A. S. (2000) Mutational, kinetic, and NMR studies of the roles of conserved glutamate residues and of Lys-39 in the mechanism of the MutT pyrophosphohydrolase, *Biochemistry 39*, 1655−1674.
6. Bessman, M. J., Frick, D. N., and O'Handley, S. F. (1996) The MutT proteins or "nudix" hydrolases, a family of versatile, widely distributed "housecleaning" enzymes, *J. Biol. Chem. 271*, 25059−25062.
7. Maki, H., and Sekiguchi, M. (1992) MutT protein specifically hydrolyzes a potent mutagenic substrate for DNA synthesis, *Nature 355*, 273−275.
8. Shibutani, S., Takeshita, M., and Grollman, A. P. (1991) Insertion of specific bases during DNA synthesis past the oxidation damaged base 8-oxodG, *Nature 349*, 431−434.
9. Cheng, K. C., Cahill, D. S., Kasai, H., Nishimura, S., and Loeb, L. A. (1992) 8-Hydroxyguanine, an abundant form of oxidative DNA damage causes G→T and A→C substitutions, *J. Biol. Chem. 267*, 166−172.
10. Treffers, H. P., Spinelli, V., and Belser, N. O. (1954) A new factor (or mutator gene) influencing mutation rates in *Escherichia coli*, *Proc. Natl. Acad. Sci. U.S.A. 40*, 1064−1071.
11. Yanofsky, C., Cox, E. C., and Horn, V. (1966) The unusual mutagenic specificity of an *E. coli* mutator gene, *Proc. Natl. Acad. Sci. U.S.A. 55*, 274−281.
12. Tsuzuki, T., Egashira, A., Igarashi, H., Iwakuma, T., Nakatsuru, Y., Tominaga, Y., Kawate, H., Nakao, K., Nakamura, K., Ide, F., Kura, S., Nakabeppu, Y., Katsuki, M., Ishikawa, T., and Sekiguchi, M. (2001) Spontaneous tumorigenesis in mice defective in the MTH1 gene encoding 8-oxo-dGTPase, *Proc. Natl. Acad. Sci. U.S.A. 98*, 11456−11461.
13. Tassotto, M. L., and Mathews, C. K. (2002) Assessing the metabolic function of the MutT 8-oxo-dGTPase in *Escherichia coli* by nucleotide pool analysis, *J. Biol. Chem. 277*, 15807−15812.
14. Massiah, M. A., Saraswat, V., Azurmendi, H. F., and Mildvan, A. S. (2003) Solution structure and NH exchange studies of the MutT pyrophosphohydrolase complexed with Mg^{2+} and 8-oxo-dGMP, a tightly bound product, *Biochemistry 42*, 10140−10154.
15. Frick, D. N., Weber, D. J., Abeygunawardana, C., Gittis, A. G., Bessman, M. J., and Mildvan, A. S. (1995) NMR studies of the conformations and location of nucleotides bound to the *Escherichia coli* MutT enzyme, *Biochemistry 34*, 5577−5586.
16. Saraswat, V., Massiah, M. A., Azurmendi, H. F., and Mildvan, A. S. (2003) NMR and mutagenesis studies of the structure of the MutT-Mg^{2+}-8-oxo-dGMP complex, *Biochemistry 42*, 8616.
17. Abeygunawardana, C., Weber, D. J., Frick, D. N., Bessman, M. J., and Mildvan, A. S. (1993) Sequence specific assignments of the backbone ^{1}H, ^{13}C, and ^{15}N resonances of the MutT enzyme by heteronuclear multidimensional NMR, *Biochemistry 32*, 13071−13080.
18. Frick, D. N., Weber, D. J., Gillespie, J. R., Bessman, M. J., and Mildvan, A. S. (1994) Dual divalent cation requirement of the MutT dGTPase, *J. Biol. Chem. 269*, 1794−1803.
19. Dawson, R. M. C., Eliot, D. C., Eliot, W. H., and Jones, K. M. (1986) *Data for Biochemical Research*, p 105, Oxford University Press, New York.
20. Trilink Biotechnologies, Inc. (1999) San Diego (product data sheet).
21. Kay, L. E., Keifer, P., and Saarinen, T. (1992) Pure absorption gradient enhanced heteronuclear single quantum coherence spectroscopy with improved sensitivity, *J. Am. Chem. Soc. 114*, 10663−10665.
22. Delaglio, F., Grzesiek, S., Vuister, G. W., Zhu, G., Pfeifer, J., and Bax, A. (1995) A multidimensional spectral processing system based on Unix Pipes, *J. Biomol. NMR 6*, 277−293.
23. Goddard, T. D., and Kneller, D. G. (2002) *SPARKY 3*, University of California, San Francisco.
24. Bai, Y., Milne, J. S., Mayne, L., and Englander, S. W. (1993) Protein stability parameters measured by hydrogen exchange, *Proteins: Struct., Funct., Genet. 17*, 75−86.
25. Rebholz, K. L., and Northrop, D. B. (1995) Kinetics of iso mechanisms, *Methods Enzymol. 249*, 211−240.
26. Mildvan, A. S., Weber, D. J., and Kuliopulos, A. (1992) Quantitative interpretations of double mutations of enzymes, *Arch. Biochem. Biophys. 294*, 327−340.
27. Sakai, Y., Furuichi, M., Takahashi, M., Mishima, M., Iwai, S., Shirakawa, M., and Nakabeppu, Y. (2002) A molecular basis for the selective recognition of 2-hydroxydATP and 8-oxo-dGTP by human MTH1, *J. Biol. Chem. 277*, 8579−8587.
28. Bruner, S. D., Norman, D. P. G., and Verdine, G. L. (2000) Structural basis for recognition and repair of the endogenous mutagen 8-oxoguanine in DNA, *Nature 403*, 859−866.
29. Fromme, J. C., and Verdine, G. L. (2002) Structural insights into lesion recognition and repair by the bacterial 8-oxoguanine DNA glycosylase, *Nat. Struct. Biol. 9*, 544−552.
30. Mahuren, J. D., Coburn, S. P., Slominski, A., and Wortsman, J. (2001) Microassay of phosphate provides a general method for measuring the activity of phosphatases using physiological, nonchromogenic substrates such as lysophosphatidic acid, *Anal. Biochem. 298*, 241−245.

BI030216O